



HHS Public Access

Author manuscript

J Mol Cell Cardiol. Author manuscript; available in PMC 2016 April 01.

Published in final edited form as:

J Mol Cell Cardiol. 2015 April ; 81: 81–93. doi:10.1016/j.yjmcc.2015.01.013.

Mechanism of automaticity in cardiomyocytes derived from human induced pluripotent stem cells

Jong J. Kim^{1,2}, Lei Yang³, Bo Lin³, Xiaodong Zhu⁴, Bin Sun², Aaron D. Kaplan⁵, Glenna C.L. Bett^{5,6,7}, Randall L. Rasmusson^{5,6}, Barry London⁴, and Guy Salama^{1,2,8}

¹Department of Bioengineering, University of Pittsburgh, Pittsburgh, PA 15261

²Department of Medicine, University of Pittsburgh, Pittsburgh, PA 15261

³Department of Developmental Biology, University of Pittsburgh, Pittsburgh, PA 15261

⁴University of Iowa, Carver College of Medicine, Division of Cardiovascular Medicine, Iowa City, IA 52242

⁵Center for Cellular and Systems Electrophysiology, University at Buffalo, State University of New York, Buffalo NY 14214

⁶Department of Physiology and Biophysics, University at Buffalo, State University of New York, Buffalo NY 14214

⁷Department of Gynecology-Obstetrics, University at Buffalo, State University of New York, Buffalo NY 14214

Abstract

Background and Objectives—The creation of cardiomyocytes derived from human induced pluripotent stem cells (hiPS-CMs) has spawned broad excitement borne out of the prospects to diagnose and treat cardiovascular diseases based on personalized medicine. A common feature of hiPS-CMs is their spontaneous contractions but the mechanism(s) remain uncertain.

Methods—Intrinsic activity was investigated by the voltage-clamp technique, optical mapping of action potentials (APs) and intracellular Ca^{2+} (Ca_i) transients (Ca_iT) at subcellular-resolution and pharmacological interventions.

Results—The frequency of spontaneous Ca_iT (s Ca_iT) in monolayers of hiPS-CMs was not altered by ivabradine, an inhibitor of the pacemaker current, I_f despite high levels of HCN transcripts (1–4). HiPS-CMs had negligible I_f and I_{K1} (inwardly-rectifying K^+ -current) and a minimum diastolic potential of $-59.1 \pm 3.3\text{mV}$ ($n=18$). APs upstrokes were preceded by a

© 2015 Published by Elsevier Ltd.

⁸To whom all correspondence should be addressed: Guy Salama, Ph.D., Department of Medicine, University of Pittsburgh, School of Medicine, 3550 Terrace Street, Suite S628 Scaife Hall, Pittsburgh, PA 15261, Tel: 412 648-9354, Fax: 412-648-5991, gsalama@pitt.edu.

The authors have no conflicts to declare

Publisher's Disclaimer: This is a PDF file of an unedited manuscript that has been accepted for publication. As a service to our customers we are providing this early version of the manuscript. The manuscript will undergo copyediting, typesetting, and review of the resulting proof before it is published in its final citable form. Please note that during the production process errors may be discovered which could affect the content, and all legal disclaimers that apply to the journal pertain.

depolarizing-foot coincident with a rise of Ca_i . Subcellular Ca_i wavelets varied in amplitude, propagated and died-off; larger Ca_i -waves triggered cellular sCaTs and APs. SCA_iTs increased in frequency with $[Ca^{2+}]_{out}$ (0.05-to-1.8mM), isoproterenol (1 μ M) or caffeine (100 μ M) (n = 5, p<0.05). hiPS-CMs became quiescent with ryanodine receptor stabilizers (K201=2 μ M); tetracaine; Na-Ca exchange (NCX) inhibition (SEA0400=2 μ M); higher $[K^+]_{out}$ (5 \rightarrow 8mM), and thiol-reducing agents but could still be electrically stimulated to elicit Ca_i Ts. Cell-cell coupling of hiPS-CM in monolayers was evident from connexin-43 expression and Ca_i T propagation. SCA_iTs from an ensemble of dispersed hiPS-CMs were out-of-phase in but became synchronous through the outgrowth of inter-connecting microtubules.

Conclusions—Automaticity in hiPS-CMs originates from a Ca^{2+} -clock mechanism involving Ca^{2+} cycling across the sarcoplasmic reticulum linked to NCX to trigger APs.

Keywords

Human myocytes from stem cells; Spontaneous activity; Subcellular Calcium waves; Funny current; Optical mapping of Calcium and action potentials; Cell-cell coupling

Introduction

A milestone of stem cell biology has been the generation of embryonic stem (ES) cells from human blastocysts [1, 2] and their differentiation into cells of all three germ layers including cardiomyocytes (CMs).[3, 4] Embryoid bodies (EBs) consisting of myocytes derived from human ES cells (hES-CMs) have the ultra-structural, electrical and Ca^{2+} cycling properties of early-stage or developing myocytes.[3, 5] In contrast to mature ventricular myocytes, hES-CMs (20–35 days post-differentiation) exhibit spontaneous excitability and contractions which were attributed to hyperpolarization- activated cyclic nucleotide-gated (HCN) channels or the pacemaker current, I_f that triggered voltage-gated Na^+ channels and current (I_{Na}) to elicit action potentials. [6] Evidence of their immature phenotype includes a notable absence of Kir2.1 (the channel protein that encodes for the inward rectifying K^+ current, I_{K1}) and a lack of functional sarcoplasmic reticulum (SR) network. [5, 6] Enhanced expression of Kir2.1 in cultured hES-CMs ablated the pro-arrhythmic action potential traits. [7] Based on action potential recordings from EBs, hES-CMs are heterogeneous in their cell type and consist of a mixture of nodal, atrial and ventricular-like myocytes.[8]

The reprogramming of human fibroblasts into induced pluripotent stem cells (hiPSCs) [9, 10] has made it possible to generate patient specific iPSCs from a readily accessible source of cells. hiPSCs possess similar proliferative properties to hESCs and the potential to differentiate into CMs. CMs derived from human iPSCs (hiPS-CMs) are genetically identical to the native donor CMs, avoid possible immune response in clinical applications and ethical concerns faced by the procurement of hESCs. HiPS-CMs are comparable to hES-CMs with similar differentiation pattern, action potential properties, distribution of cell types (nodal, atrial and ventricular) and responses to α - and β -adrenergic stimulation.[11–14] HiPS-CMs generated from patients with LEOPARD [15] or long QT syndrome [16, 17] were shown to retain the expected characteristics of the patients' cardiac phenotypes, demonstrating great promise for patient specific diagnostics and treatments.[14, 17, 18]

Studies of Ca^{2+} handling in hES-CMs and hiPS-CMs have yielded contradictory results. Studies reported a lack of contractile response to ryanodine and thapsigargin and a relatively immature SR function in hES-CMs,[5, 19] or functional SR but with an immature Ca^{2+} cycling phenotype in 38% of hES-CMs[20] or operative Ca^{2+} -induced Ca^{2+} release despite a leaky SR in hES-CMs enriched for ventricular-like cells.[21] A study of pacemaker mechanisms in hES-CMs (11–21 days post-EB formation) found marked heterogeneities of action potential shape and pacemaker properties yet all cells had substantial I_f levels.[22] Spontaneous activity was reduced by I_f inhibitors in some but not all cells while other cells responded to Na-Ca exchange (NCX) inhibitors and still others responded to both types of inhibitors, suggesting that voltage and Ca^{2+} clock mechanisms can co-exist. Blockade of both I_f and I_{NCX} did not eliminate pacemaker activity and the residual pacemaker current was attributed to the turn-off of Ca^{2+} activated K^+ channels ($I_{\text{KCa}}/\text{SK4}$). Overexpression of SK4 channels in embryonic stem cells leads to an increase in pacemaker cell differentiation emphasizing its importance in the early development of the conduction system. [23] A comparison of Ca^{2+} handling properties of hES-CMs and hiPS-CMs reported that iPS-CMs have smaller amplitude and slower Ca^{2+} kinetics than hES-CMs suggesting that 20-days old hiPS-CMs are more immature than hES-CMs.[24] Others found that hiPS-CMs have Ca^{2+} cycling properties of adult ventricular myocytes [25] and hiPS-CMs generated from a CPVT (catecholaminergic polymorphic ventricular tachycardia) patient carrying a mutation in RyR2 (cardiac ryanodine receptor) recapitulated the Ca^{2+} signaling phenotype of the CPVT syndrome.[25, 26] Despite these inconsistencies about Ca^{2+} cycling properties, spontaneous contractions of CMs are commonly used as evidence of successful differentiation to cardiomyocytes from pluripotent stem cells. Yet, the mechanisms underlying automaticity have not been systematically investigated making it difficult for hiPS-CMs to reach their full potential as a therapeutic tool.

Here, we studied the mechanisms underlying spontaneous electrical and mechanical activity (through changes in Ca^{2+} transients: CaT) of cultured hiPS-CMs using optical mapping of action potentials (APs) and CaT and using the whole-cell voltage-clamp technique. CaT were measured using low (Rhod-2/AM, $K_D = 500$ nM) [27] and high (GCaMP2; $K_D=146$ nM [28] affinity Ca^{2+} sensors to insure the detection of low amplitude intracellular Ca^{2+} (Ca_i) signals in monolayers of hiPS-CMs and single cells. Ionic and pharmacological interventions were applied to show that a Ca^{2+} -clock mechanism involving Ca^{2+} cycling across the sarcoplasmic reticulum (SR) linked to membrane potential changes via the sodium-calcium exchanger (NCX) is responsible for their spontaneous activity.

Methods

Maintenance and cardiomyocyte differentiation of human iPS cells

A human Y1 iPS cell line was generated from human fibroblast line HDF- α and were fully characterized as previously described.[29] The following conditions were used for cardiomyocyte differentiation[30] from Y1 iPSCs by forming EBs using the basal StemPro®-34 medium (Invitrogen) as described in our previous studies[29, 30]: days 0–1, BMP4 (5 ng/ml); days 1–4, BMP4 (10 ng/ml), bFGF (5 ng/ml) and Activin (1.5 ng/ml); days 4–20, DKK1 (150 ng/ml) and VEGF (10 ng/ml). Cultures were maintained in a 5%

CO₂/5% O₂/90% N₂ environment for the first 20-days and were then transferred into a 5% CO₂/air environment. All cytokines were purchased from R&D Systems. To study dissociated hiPS-CMs, spontaneously beating EBs were dissociated by incubation with 1mg/ml collagenase B for 30 min at 37 °C, followed with 0.25% trypsin for 5 min at 37 °C, and then plated on laminin-coated cover slips or dishes. The purity of our hiPS-CMs was previously shown to be >80%. [31]

Optical Mapping of Human iPS-CMs

Cells were loaded with Rhod-2/AM [32] or infected with AAV-GCaMP2 to measure intracellular Ca²⁺ (Ca_i)[33] and/or stained with di-4-ANEPPS or Pittsburgh1 (PGHI) to measure voltage.[34] Cells were allowed to anchor on laminin coated plasticware and were placed on the heated stage of an Olympus BX1f microscope. Optical mapping was performed at high spatiotemporal resolution (100 × 100 pixels, 150 μm × 150 μm; 100 Hz) at 37°C using two SciMedia CMOS cameras (Ultima One) with a 100×100 pixel, as previously described.[35] Excitation light intensity was carefully adjusted not to cause cell damage due to phototoxicity. Membrane potential (V_m) and intracellular Ca²⁺ (Ca_i) were simultaneously measured in spontaneously beating hiPS-CM clusters or single cells followed by various ionic or pharmacological interventions to manipulate automaticity. K201 (3-(4-Benzylcyclohexyl)-1-(7-methoxy-2, 3-dihydrobenzo[*f*][1,4]thiazepin-4(5*H*)-yl)propan-1-one) was synthesized and generously provided by Dr. Robert Strongin and Dr. Jonathan Abramson (Portland State University). SEA0400 was the generous gift of Dr. András Varró and Dr. Norbert L. Iost (University of Szeged). Field electrical shocks were applied to pace iPS-CMs.

Calcium mapping of hiPS-CMs with genetically encoded probes

Cells were genetically encoded with the Ca²⁺ sensor GCaMP2 using an adeno-associated viral vector AAV-GCaMP2 infection at MOI of 10⁵ for 48 hours, as previously described. [28]

Immunolabeling and fluorescence microscopy

HiPS-CMs were fixed in 2% paraformaldehyde in PBS, permeabilized in 0.1% Triton X-100, washed in PBS, and blocked with 2% BSA in PBS. Fixed cells were incubated with primary then secondary antibodies with extensive washings to remove unbound antibodies. Cells were imaged with an inverted Nikon Eclipse TS100 microscope using a CCD camera (Quantitative Imaging Corporation) and software from iVision (Biovision Technologies). The following antibodies were used for fluorescence microscopy: anti-human Troponin T from Lab Vision; anti-human α-Actinin from Sigma Aldrich and anti-Connexin 43/GJA1 from Abcam (1:200 dilution). Alexa 488 and Cy3- conjugated secondary antibodies were purchased from Invitrogen; slides were also stained with DAPI (Invitrogen, 1:1000 dilution) to visualize nuclei.

Electrophysiology

HiPS-CMs were seeded at a density of 20,000 – 40,000 viable cells in DMEM (Dulbecco's Modified Eagle Medium)/FBS (fetal bovine serum) media on twelve 15-mm cover-slips

coated with 0.1% (w/v) gelatin (Sigma) solution placed in 12 well plates, and incubated for at least 2 days at 37° C, 5% CO₂, before recording. Action potentials (APs) and ionic currents were recorded from single hiPS-CMs using the whole-cell patch clamp technique at room temperature using Axopatch1D, Digidata 1322A, and pClamp 9 (Axon Instruments) for data amplification, acquisition and analysis. Electronic expression of I_{K1} was applied using a Cybercye dynamic clamp system (Cytocybernetics). The electrical signature was used as a criterion to classify myocytes as either ventricular, atrial or other as previously described.[36, 37] Of 31 cells, 21 were classified as ventricular (68%), 6 as atrial (19%) and 3 as other (<1%). Micropipettes had resistances of 2–4 MΩ. Patch pipettes contained (mM): 140 KCl, 1 MgCl₂, 5 EGTA, 5 ATP (Mg²⁺ salt), 5 Na₂-creatinephosphate, 0.2 GTP, and 10 HEPES, pH 7.4. The extracellular solution contained (in mM): 144 NaCl, 5.4 KCl, 1 MgCl₂, 2.5 CaCl₂, 5.6 glucose, and 10 HEPES, pH 7.4. Total currents were obtained by applying voltage steps from –120 mV to +40 mV for 2,000 ms from a holding potential of –90 mV. I_{K1} and I_F were recorded by applying voltages ranging from –140 mV to +20 mV for a duration of 2,000 ms from a holding potential of –40 mV. Recordings were taken before and after adding 1 mM BaCl₂ to the bath solution. The I_{K1} component of the current was obtained by taking the peak barium sensitive component, by subtracting the barium treated current from the control. I_F component of the current was estimated to be negligible from the nearly linear barium insensitive current at the end of the 2,000 ms pulse.

RT-PCR

Total RNA was extracted using Qiagen RNeasy Kit. cDNA was synthesized using SuperScript II reverse transcriptase (Invitrogen), according to manufactory's instruction. Real time PCR was performed in triplicates using SYBR green PCR mix (Invitrogen). Human Cyclophilin G was used as an endogenous control. The primers used are listed in Table 1.

Results

As in our previously established methods [10], we differentiated hiPS cells into cardiomyocytes by first forming embryoid bodies (Figure 1A). Immunostaining of hiPS-CMs showed abundant expression of α-actinin, cardiac troponin T and atrial natriuretic peptide (ANP) (Figure 1). The mRNA levels for cardiac troponin T (cTNT), voltage-gated Na⁺ channel (SCN5a), nerve growth factor (NGF), and the hyperpolarization-activated, cyclic nucleotide-gated channels, isoforms 1–4 (HCN 1–4) of pacemaker channels increased following differentiation to CMs (Figure 1A, i.v.). The message levels for HCN2 and HCN4 isoforms may be most relevant to hiPS-CMs because they may underlie the fast and slow components of human cardiac I_f in the atrium and ventricle.[38] HCN2 and HCN4 were also shown to be co-localized in sinoatrial rabbit myocytes through functional interactions with the adapter protein SAP97.[39]

Simultaneous measurements of APs and intracellular free Ca²⁺ (Ca_i) were recorded using PGHI and Rhod-2/AM from clusters of spontaneously beating hiPS-CMs shown in Figure 1B. The shape and time-course of APs recorded from individual cells within the cluster had ventricular-like APs. Note that several properties are typically associated with ventricular

rather than pacemaker-like cells: 1) a stable resting potential, 2) a high AP plateau, 3) a rapid AP downstroke or 'phase 3' repolarization, and 4) a tight V_m to Ca_i (excitation-contraction) coupling. A plot of AP durations as a function of cycle length (CL) demonstrates particularly long AP durations consistent with human ventricular-like APs.

Confluent monolayers were formed after dissociating the hiPS-EBs and then seeding them on laminin-coated coverslips for 2–5 days. The hiPS-CMs in monolayers revealed an organized sarcomeric α -Actinin structure and exhibited extensive cell-cell coupling via connexin 43 (Figure 1C). Both confluent and isolated hiPS-CM(s) contracted spontaneously (supplementary movie 1 and 2, respectively). APs in beating hiPS-CMs had elevated plateau phases and long APDs that prolonged with longer cycle lengths. Automaticity was observed for up to 3 months post CM seeding.

Contributions of I_f and I_{K1} currents to automaticity in hiPS-CMs

The pacemaker potential in sinoatrial node cells has been traditionally attributed to a current activated by hyperpolarization and modulated by cAMP, called the funny current, I_f and the channel encoding HCN family of genes. The HCN2 and HCN4 isoforms may be most relevant to hiPS-CMs because they have been reported to underlie the fast and slow components of I_f in the atrium and ventricle [38] and are co-localized in sinoatrial rabbit myocytes through functional interactions with the adapter protein SAP97. [39] We showed that expression of the HCN family of genes [40] was up-regulated in beating hiPS-CMs; furthermore, a slow diastolic depolarization or pacemaker potential was occasionally (<5% of cells) recorded optically in our hiPS-CMs (supplementary Figure 1A). Thus, we tested the contribution of I_f to automaticity in our hiPS-CM clusters by adding ivabradine, a selective inhibitor of I_f to the bathing medium while recording spontaneous Ca_i Ts (s Ca_i Ts) optically. As shown in Figure 2A(i), ivabradine at relatively high concentrations of 3 and 9 μ M did not alter the rate of s Ca_i Ts ($p > 0.7$, $n = 8$ separate confluent beating hiPS-CM monolayers; Figure 2A(iii) top panel). The failure to suppress the frequency of s Ca_i Ts after I_f inhibition suggests that within the ensemble of hiPS-CMs, the cells or group of cells controlling automaticity did not rely on I_f and other factors were responsible for their spontaneous activity.

Due to concerns that ivabradine might be ineffective at blocking I_f in hiPS-CMs, alternative approaches were tested: a) titrations of extracellular $[K^+]$ ($[K^+]_{ex}$) and b) direct measurements of I_f by voltage-clamp. An accepted feature of the slow diastolic depolarization (in the range of -70 to -45 mV) is that shifts to more positive potentials via an increase in $[K^+]_{ex}$ (5 to 25 mM) results in an increase in firing rate. [41–43] As shown in Figure 2A(ii), raising $[K^+]_{ex}$ from 4 to 8 and to 12 mM accomplished the opposite effect and caused a significant decrease of s Ca_i Ts ($p < 0.01$ after 60 seconds, $n = 5$; Figure 2A(iii) bottom panel); s Ca_i Ts ceased at 12 mM $[K^+]_{ex}$.

Consistent with the ivabradine and $[K^+]_{ex}$ results, measurements of the barium sensitive and insensitive currents in the range of -140 and 0 mV revealed that I_f and I_{K1} were negligible (Figure 2B, a and b). The average current to voltage relationship for late (2000 ms) (panel a) and early (peak, panel b) currents showed the absence of inward rectification (I_{K1}) compared to adult acutely isolated human cell currents (panel c) and very small difference from the initial currents, suggestive of little or no time-dependent activation of I_f (Figure 2B). The

Ba²⁺ sensitive currents from our myocytes was similar in magnitude to those measured from commercially available iCell hiPS cells (CDI, Wisconsin). I_{K1} was extremely low density compared to adult acutely isolated human cell currents calculated from the O'Hara-Rudy model (panel d).[44]

To determine the nature of pacemaking activity in hiPS-CMs, the diastolic depolarization was measured in 18 dispersed cells under whole cell current-clamp mode. As shown in Figure 2C, two types of pacemaking activity were observed; the first (n=11/18 cells) showed a first phase of depolarization immediately following the minimum diastolic potential, followed by a typical 'flat' period prior to the initiation of an AP. Afterdepolarization preceded the AP upstrokes (arrows) typical of a spontaneous Ca²⁺ release event or 'delayed afterdepolarization' (DAD). The second type of pacemaking activity was observed less frequently (n=3/18 cells) and showed pacemaker activity with diastolic depolarization preceding action potentials. Even for these hiPS-CMs, spontaneous depolarizations consistent with DADs were observed (Figure 2C, right trace) and 4/18 cells were sufficiently depolarized to show no spontaneous activity unless stimulated.

Spontaneous SR Ca²⁺ release or non-voltage gated cytosolic Ca²⁺ elevation in hiPS-CMs

In single hiPS-CMs expressing the genetically encoded Ca²⁺ indicator, GCaMP2, spontaneous non-voltage triggered cytosolic Ca²⁺ elevations were consistently recorded (supplementary Figure 1B). The spontaneous Ca²⁺ elevations appeared typically from 2–3 sites, were out-of-phase and led to Ca_i wavelets that propagated within the cell (5–10 μm). Most subcellular Ca_i wavelets propagated locally and failed to trigger a synchronous CaT throughout the cell. However, successive Ca_i wavelets started from the same site, increased in amplitude and intermittently triggered a full amplitude cellular CaT. Figure 3A(i) illustrates fluorescence images from an isolated hiPS-CM (field-of-view = 50×50 μm²) expressing GCaMP2 and taken at various time points. Here, Ca_i elevation started at site 'a' at 0.76s, propagated to 'b' at 0.84s then 'c' at 0.92s followed by a cellular CaT at 1.5s. The next Ca_i wavelet started at site 'c' at 2.86s propagated to 'b' and 'a' at 2.96 and 3.06 s and then died off. Figure 3A(ii) shows the superposition of Ca_i traces from sites a, b and c. with box 1 equivalent to the images from 0.6 to 1.5 sand box 2 to images labeled 2.86 to 3.06s. Note that the CaT at 1.5 s is followed by two Ca_i wavelets at 3.1 and 4.8 s that die off. An expanded time-sweep of the Ca_i traces in box 1, shows that subcellular SR Ca²⁺ release from three sites (a, b and c) were out-of-phase, with site a preceding b and c and were followed by a cellular synchronous CaT (Fig. 3A-ii, Box 1). The out-of-phase Ca_i wavelets that followed the CaT at 1.5 s remained small in amplitude and did not precede a synchronous cellular CaT (Box2).

Figure 3B illustrates subcellular Ca_i wavelets in one myocyte that elicit a synchronous cellular CaT in the same cell and in an adjacent myocyte. At time-points 4.2, 4.4 to 4.66 s, Ca_i elevation starts at sites d, and propagates to site e then f where it triggers a synchronous cellular CaT (Figure 3B-i, 2nd Ca_i transient, arrow). In this case, the CaT spreads to the adjacent cell (Figure 3B panel 4.7 sec), most likely through the propagation of an AP. The superposition of Ca_i traces from sites d, e and f show the local Ca_i wavelets that are prominent in all three sites and the time-shifts of the synchronous CaT at the three sites

(Figure 3B(ii) top traces). CaTs in cell 2 follow each CaTs in cell 1 consistent with tight coupling between cell 1 and 2 (Figure 3B(ii) bottom traces).

The spontaneous Ca_i elevation in hiPS-CMs suggests a Ca^{2+} -clock mechanism as the basis of their automaticity. Experimental and computational studies have previously shown that the frequency of spontaneous Ca_i release from local Ca^{2+} release units increases with increasing external Ca^{2+} due to greater SR Ca^{2+} loads. [45] As shown in Figure 4A, the frequency of spontaneous activity of hiPS-CMs was dependent on the external Ca^{2+} concentrations ($[\text{Ca}^{2+}]_o$). In these preparations, $[\text{Ca}^{2+}]_o$ was systematically increased and then decreased to demonstrate that changes in $[\text{Ca}^{2+}]_o$ changed the incidence of stochastic Ca_i waves, the amplitude of CaT and controlled automaticity (n=4). The analysis exposed a statistically significant correlation between $[\text{Ca}^{2+}]_o$ and frequency of spontaneous activity (Figure 4A right boxplot).

Figure 4B illustrates an example of spontaneous Ca_i transients before and after β 1-adrenergic stimulation with isoproterenol (1 μM). As in adult myocytes, isoproterenol increased the rate of spontaneous activity in all hiPS-CM preparations (n=4/4). Intriguingly, isoproterenol promoted diastolic Ca^{2+} elevations (arrows, Figure 4B, bottom trace) were increased in incidence and amplitude to increase the frequency of automaticity. The chronotropic response implicates a role for SR Ca^{2+} release and re-uptake via SERCA pumps in hiPS-CMs. The presence of functional SR in hiPS-CMs was tested by the additions of 100 or 500 μM caffeine in the medium which is known to activate RyR2 opening and cause SR Ca^{2+} release. Low dose of caffeine increased basal Ca^{2+} and automaticity, while a high dose lead to SR Ca^{2+} release (Figure 4C).

Additional experiments were carried out to characterize the Ca^{2+} handling properties of hiPS-CMs. The RyR2 stabilizer, K201 gradually suppressed the rate of spontaneous activity of hiPS-CMs (n=4/4) until the cells became quiescent; of note, the cells could still be stimulated to fire APs and CaT (Figure 5A). K201 at 2 μM has negligible off-target effects. Tetracaine, an inhibitor of RyR2, and ryanodine were also tested to determine if spontaneous activity relied on spontaneous SR Ca^{2+} release via RyR2 opening. Tetracaine (5 μM) reduced the rate (Figure 5B) and ryanodine (10 μM) abolished spontaneous activity in hiPS-CMs (not shown).

More recent studies have attributed the pacemaker to the forward mode of the Na-Ca exchanger (NCX) which links a Ca^{2+} clock mechanism consisting of Ca^{2+} cycling by the SR to rhythmical changes in membrane potential.[45] Figure 5C shows that inhibition of NCX with SEA0400 (2 μM) gradually slowed down and eventually arrested automaticity (n=4/4).

The oxidation-reduction state of critical sulfhydryl groups is known to regulate SR Ca^{2+} release via RyR2 where thiol oxidizing agents promote channel opening and reducing agents promotes its closure and interruption of SR Ca^{2+} -leaks.[46–48] Addition of the membrane permeable reducing agents N-Acetyl-L cysteine (NAC=10 mM) to hiPS-CMs for 5 minutes reduced the rate of spontaneous activity (Figure 6A). Similar findings were obtained with 1 mM ascorbic acid (AA). Captopril was shown to act as a membrane permeable thiol reducing agent that decreases the open probability (P_o) of RyR2.[48] As shown in Figure

6B, Captopril (1mM) slowed down the rate of spontaneous CaT in minutes and interrupted automaticity within 15 min (4 out of 8 beating clusters). In the presence of captopril, contractions could still be triggered by electrical pacing (lower panel). Similar results were obtained with other sulfhydryl reducing agents (dithiothreitol, DTT=1 mM, not shown). Although NAC and captopril are nonselective sulfhydryl reducing agents, these findings suggest that RyR2 are particularly prone to thiol oxidation resulting in an increase in the open probability (P_o) of RyR2 and leakier RyR2, which enhances spontaneous Ca^{2+} release.

Subcellular Ca^{2+} waves could be responsible for the automaticity, but it is unclear how subcellular calcium waves synchronize spontaneous intercellular contractions. Clusters of hiPS-CMs and individual cells within the cluster were highly synchronized and exhibited stable rates of contraction (Figure 7A, supplementary movie 3). In dispersed CMs, contractions were highly irregular and adjacent cells contracted out-of-phase (Figure 7B, supplementary movie 4). In time, synchronization improved and propagation of contraction was observed in large cluster of iPS-CMs which became eventually tightly coupled. In a dense cluster of hiPS-CMs, intercellular synchronization and propagation of electrical wave are likely mediated by gap junctions, consistent with the high levels of connexin 43 expression (Cx43, Figure 1C). Intriguingly, intercellular synchronization of spontaneous contraction was occasionally observed in remote hiPS-CMs that were over 200 μ m apart (Figure 7C, panel a, supplementary movie 5). High resolution optical imaging on sparsely distributed hiPS-CMs stained with a membrane-bound voltage sensitive dye revealed a complex intercellular network of microfibers (Figure 7C, panel c). Intercellular synchronization between dispersed cells was observed through the synchronization of Ca_i transients and hiPS-CM interconnections via micro-tubules (Figure 7C panels a and b). Cell-cell coupling implies that in an ensemble of hiPS-CMs, the spontaneous pacemaker activity of the cell with the fastest beating rate controls the rate of contractions and automaticity of the ensemble. In a coupled ensemble, synchronization is mediated by the propagation of APs and the AP upstroke will precede the rise of Ca_i except in the fastest cell that controls automaticity. As a cautionary note, cell-cell coupling of seemingly remote cells should be carefully considered in voltage-clamp experiments to avoid loss of spatial voltage control.

Table 1S in the supplement summarizes the statistical analysis for each intervention presented in this study.

Discussion

In adult hearts, voltage-gated Ca^{2+} cycling is an essential component of the initiation of cardiac contraction and the regulation of cardiac gene expression via various Ca^{2+} -dependent signaling pathways. Such Ca^{2+} signaling is also involved in cardiac cell growth and functional maturation during early embryonic stages of cardiomyocytes. Experimentally, the suppression of Ca^{2+} entry via L-type Ca^{2+} channels (LTCCs), as a consequence of deletion of the α_1 subunit of LTCCs, results in poor cell growth and failed chamber formation during embryogenesis.[49] Similarly, in engineered 3D cardiac tissues (utilizing iPS-CMs), forced contraction (by electrical stimulation) was beneficial for their structural and functional maturation.[50] Thus, spontaneous contractions in immature iPS-

CMs may play a critical role in their functional and structural maturation, even in non-pacemaker cells.

In sinoatrial nodal or pacemaker cells, the mechanisms underlying automaticity remain somewhat controversial with two competing mechanisms that have been proposed to explain pacemaker activity: a) “voltage clock” driven by the activation of I_f at negative membrane potentials ($-60/-70$ mV), or b) a “ Ca^{2+} clock” consisting of Ca^{2+} cycling across the SR linked to membrane currents via I_{NCX} . [40, 51] Considerable evidence was presented in favor of both mechanisms leading to the conclusion that they are not mutually exclusive and both partake in rhythm regulation. [52]

Automaticity in hiPS-CMs

One possible mechanism is that an inward current generated by I_f is responsible for a slow diastolic depolarization and when the voltage reaches the threshold potential of L-type Ca^{2+} channels, the activation of $I_{\text{Ca,L}}$ initiates a ‘ Ca^{2+} ’ action potential and automaticity. The HCN family, which encodes for I_f , are not only expressed in SA node cells but are prominently found in ventricular myocytes of newborn rat hearts and in pathological conditions such as mild to severe hypertrophy and following myocardial infarction. [53–55] In human ventricular myocytes, HCN4 and HCN2 mRNA levels are readily detected (HCN4 > HCN2) but the funny current, I_f is barely detectable, except in hypertrophic ventricular myocytes where mRNA and I_f are markedly upregulated. [53, 56]

Spontaneous activity of embryoid bodies or dispersed cardiomyocytes from hiPS-CMs occurred in cells with ventricular-like APs (e.g. long durations and prominent plateau phases) that differ markedly from the AP of SA node pacemaker cells. However, in an ensemble of synchronously beating hiPS-CMs, it is possible that one or more cells with I_f currents maintain the spontaneous activity of the group irrespective of whether or not the cells exhibit SA node-like or ventricular-like action potentials. However, we found that although expression levels of HCN family was moderately elevated, I_f was not responsible for automaticity in clusters of hiPS-CMs because ivabradine did not alter the rate of spontaneous activity, even at high concentrations; at 3 and 9 μM ivabradine, I_f is expected to be blocked by ~67% and >80% respectively. [57] Consistent with the lack of ivabradine response, I_f density was not measurable in any of the cells that were voltage-clamped ($n=19$). Pacemaker mechanisms in hES-CMs [22] are in sharp contrast to our findings in hiPS-CMs where I_f was not detected and I_f inhibition did not alter pacemaker activity.

Automaticity can also be promoted by suppressing I_{K1} which in adult working myocardium results in spontaneous AP generation. Such a mechanism also contributes to automaticity in ES-CMs where I_{K1} is negligible due to the down regulation of KCNJ2 expression, which encodes for inwardly-rectifying K^+ channels. The loss of I_{K1} reduces the K^+ conductance and shifts the resting potential to more positive values, rendering the cells more excitable and more prone to spontaneous activity. Consistent with this mechanism, the forced expression of Kir2.1 in ES-CMs [7] or the electronically expressed I_{K1} in hiPS-CMs [36] increased I_{K1} and suppressed spontaneous AP firing. Here we showed that I_{K1} in hiPS-CMs was minimal which makes these cells prone to spontaneous activity, requiring a relatively small depolarizing current to reach the threshold potential of Na^+ or Ca^{2+} channels and

thereby trigger an AP. Such a depolarizing current can be provided by a spontaneous release of Ca^{2+} from the SR, causing an elevation of cytosolic Ca^{2+} , activation of the forward mode of the sodium-calcium exchanger (NCX), an inward I_{NCX} depolarizing current and an AP.

Several lines of evidence support spontaneous SR Ca^{2+} release as the controlling mechanism of automaticity in hiPS-CMs: 1) Subcellular optical recording of Ca^{2+} reveals frequent non-voltage triggered local Ca^{2+} waves that propagate and die-off, with larger amplitude Ca_i waves precede a spontaneous beat. 2) Increasing external Ca^{2+} systematically increased the frequency of spontaneous activity by increasing cellular Ca^{2+} , accelerating SR Ca^{2+} uptake and release and thereby speeding the Ca^{2+} -clock.[45] 3) An increase of external $[\text{K}^+]_o$ slowed-down and then stopped spontaneous activity, a finding consistent with a Ca^{2+} clock rather than an I_f -mediated mechanism since high $[\text{K}^+]$ tends to increase the Na^+ conductance of HCN channels and the rate of AP firing in pacemaker cells.[42] 4) K201 (2 μM), a selective stabilizer of the cardiac ryanodine receptor (RyR2), [58] inhibited spontaneous SR Ca^{2+} release, intracellular Ca^{2+} waves and spontaneous activity. 5) Ryanodine or caffeine or inhibition of I_{NCX} interrupted SR Ca^{2+} cycling and stopped spontaneous activity which indicates that Ca_i elevation and the associated increase in I_{NCX} generate spontaneous activity.

It is unclear why the frequency of automaticity varies in different preparations of hiPS-CMs; but a few hypotheses emerge from the data. Reactive oxygen species (ROS) and the subsequent increase in oxidative stress have traditionally been attributed to cause pathogenesis of cardiovascular disease such as cardiac hypertrophy and fibrosis in adult mammalian hearts.[59] However, recent experimental studies revealed that moderate degree of ROS activity, which mediates diverse signaling pathways, is an essential compartment of developmental process of cardiomyocytes. Furthermore, ROS is specifically known to contribute to genomic stability of stem cell derived CMs. Once ROS activity is augmented in SC-CMs, it can activate CaMKII, which augments I_{Na} and I_{CaL} and eventually leads to intracellular Na^+ and Ca^{2+} overload.[60] In turn, ROS-mediated hyperactivity of CaMKII can directly increase P_o of RyR2 which in combination with CaMKII-mediated SR Ca^{2+} overload can facilitate spontaneous SR Ca^{2+} release and automaticity.[61] The immature structure of troponin C in early stage of hiPS-CMs could reduce cytosolic Ca^{2+} buffering to facilitate SR Ca^{2+} loading and spontaneous SR Ca^{2+} release.

The current data provides compelling evidence that in hiPS-CMs automaticity is caused by spontaneous SR Ca^{2+} release which activates the Na-Ca exchanger which in the forward mode provides the depolarizing current needed to trigger an action potential. Hence, hiPS-CMs with a ventricular-like phenotype lacking typical pacemaker properties can drive automaticity. The pharmacological and ionic interventions applied in these experiments indicate that these cells have a functional SR. These findings improve our understanding of Ca^{2+} handling in hiPS-CMs, a necessary step towards the development of patient-specific cell based therapies.

Supplementary Material

Refer to Web version on PubMed Central for supplementary material.

Acknowledgments

Thanks are due to Shanping Shi for technical assistance; the study was supported by a Three Rivers Affiliate of the American Heart Association (AHA) Pre-Doctoral Fellowship to Dr. Jong J. Kim, AHA SDG Grant (#11SDG5580002) to L.Y., AHA GIA to RLR and grants from the National Heart and Lung Institute, NHLBI, HL093631 to GCLB, HL062465 to RLR, NIH DP1OD003819 to BL, and HL70722 and HL093074 to GS.

Glossary

iPSC	inducible pluripotent stem cells
CM	cardiomyocytes
hiPS-CMs	human cardiomyocytes derived from iPS cells
ESCs	embryonic stem cells
hESCs	human ESCs
Ca_i	intracellular Ca ²⁺
SR	sarcoplasmic reticulum
APs	action potentials
Ca_iT	intracellular Ca ²⁺ transients
RyR2	cardiac ryanodine receptor
K201	(1,4-benzothiazepine)
NCX	sodium-calcium exchanger
DTT	dithiothreitol
SAN	sinoatrial node
CX43	connexin 43
I_f	funny current
I_{K1}	inwardly rectifying K ⁺ -current
HCN	hyperpolarization-activated cycling nucleotide-gated channel

References

1. Thomson JA, Itskovitz-Eldor J, Shapiro SS, Waknitz MA, Swiergiel JJ, Marshall VS, et al. Embryonic stem cell lines derived from human blastocysts. *Science*. 1998; 282:1145–7. [PubMed: 9804556]
2. Reubinoff BE, Pera MF, Fong CY, Trounson A, Bongso A. Embryonic stem cell lines from human blastocysts: somatic differentiation in vitro. *Nat Biotechnol*. 2000; 18:399–404. [PubMed: 10748519]
3. Kehat I, Kenyagin-Karsenti D, Snir M, Segev H, Amit M, Gepstein A, et al. Human embryonic stem cells can differentiate into myocytes with structural and functional properties of cardiomyocytes. *J Clin Invest*. 2001; 108:407–14. [PubMed: 11489934]
4. Itskovitz-Eldor J, Schuldiner M, Karsenti D, Eden A, Yanuka O, Amit M, et al. Differentiation of human embryonic stem cells into embryoid bodies compromising the three embryonic germ layers. *Mol Med*. 2000; 6:88–95. [PubMed: 10859025]

5. Dolnikov K, Shilkrut M, Zeevi-Levin N, Gerecht-Nir S, Amit M, Danon A, et al. Functional properties of human embryonic stem cell-derived cardiomyocytes: intracellular Ca²⁺ handling and the role of sarcoplasmic reticulum in the contraction. *Stem Cells*. 2006; 24:236–45. [PubMed: 16322641]
6. Satin J, Kehat I, Caspi O, Huber I, Arbel G, Itzhaki I, et al. Mechanism of spontaneous excitability in human embryonic stem cell derived cardiomyocytes. *J Physiol*. 2004; 559:479–96. [PubMed: 15243138]
7. Lieu DK, Fu JD, Chiamvimonvat N, Tung KC, McNerney GP, Huser T, et al. Mechanism-based facilitated maturation of human pluripotent stem cell-derived cardiomyocytes. *Circ Arrhythm Electrophysiol*. 2013; 6:191–201. [PubMed: 23392582]
8. He JQ, Ma Y, Lee Y, Thomson JA, Kamp TJ. Human embryonic stem cells develop into multiple types of cardiac myocytes: action potential characterization. *Circ Res*. 2003; 93:32–9. [PubMed: 12791707]
9. Yu PB, Deng DY, Lai CS, Hong CC, Cuny GD, Boussein ML, et al. BMP type I receptor inhibition reduces heterotopic [corrected] ossification. *Nat Med*. 2008; 14:1363–9. [PubMed: 19029982]
10. Takahashi K, Tanabe K, Ohnuki M, Narita M, Ichisaka T, Tomoda K, et al. Induction of pluripotent stem cells from adult human fibroblasts by defined factors. *Cell*. 2007; 131:861–72. [PubMed: 18035408]
11. Gai H, Leung EL, Costantino PD, Aguila JR, Nguyen DM, Fink LM, et al. Generation and characterization of functional cardiomyocytes using induced pluripotent stem cells derived from human fibroblasts. *Cell Biol Int*. 2009; 33:1184–93. [PubMed: 19729070]
12. Yokoo N, Baba S, Kaichi S, Niwa A, Mima T, Doi H, et al. The effects of cardioactive drugs on cardiomyocytes derived from human induced pluripotent stem cells. *Biochem Biophys Res Commun*. 2009; 387:482–8. [PubMed: 19615974]
13. Zwi L, Caspi O, Arbel G, Huber I, Gepstein A, Park IH, et al. Cardiomyocyte differentiation of human induced pluripotent stem cells. *Circulation*. 2009; 120:1513–23. [PubMed: 19786631]
14. Zhang J, Wilson GF, Soerens AG, Koonce CH, Yu J, Palecek SP, et al. Functional cardiomyocytes derived from human induced pluripotent stem cells. *Circ Res*. 2009; 104:e30–41. [PubMed: 19213953]
15. Carvajal-Vergara X, Sevilla A, D'Souza SL, Ang YS, Schaniel C, Lee DF, et al. Patient-specific induced pluripotent stem-cell-derived models of LEOPARD syndrome. *Nature*. 2010; 465:808–12. [PubMed: 20535210]
16. Itzhaki I, Maizels L, Huber I, Zwi-Dantsis L, Caspi O, Winterstern A, et al. Modelling the long QT syndrome with induced pluripotent stem cells. *Nature*. 2011; 471:225–9. [PubMed: 21240260]
17. Matsa E, Rajamohan D, Dick E, Young L, Mellor I, Staniforth A, et al. Drug evaluation in cardiomyocytes derived from human induced pluripotent stem cells carrying a long QT syndrome type 2 mutation. *Eur Heart J*. 2011; 32:952–62. [PubMed: 21367833]
18. Priori SG. Induced Pluripotent Stem Cell-Derived Cardiomyocytes and Long QT Syndrome: Is Personalized Medicine Ready for Prime Time? *Circ Res*. 2011; 109:822–4. [PubMed: 21960720]
19. Binah O, Dolnikov K, Sadan O, Shilkrut M, Zeevi-Levin N, Amit M, et al. Functional and developmental properties of human embryonic stem cells-derived cardiomyocytes. *Journal of electrocardiology*. 2007; 40:S192–6. [PubMed: 17993321]
20. Liu J, Fu JD, Siu CW, Li RA. Functional sarcoplasmic reticulum for calcium handling of human embryonic stem cell-derived cardiomyocytes: insights for driven maturation. *Stem Cells*. 2007; 25:3038–44. [PubMed: 17872499]
21. Li S, Cheng H, Tomaselli GF, Li RA. Mechanistic basis of excitation-contraction coupling in human pluripotent stem cell-derived ventricular cardiomyocytes revealed by Ca²⁺ spark characteristics: direct evidence of functional Ca²⁺-induced Ca²⁺ release. *Heart Rhythm*. 2014; 11:133–40. [PubMed: 24096168]
22. Weisbrod D, Peretz A, Ziskind A, Menaker N, Oz S, Barad L, et al. SK4 Ca²⁺ activated K⁺ channel is a critical player in cardiac pacemaker derived from human embryonic stem cells. *Proc Natl Acad Sci U S A*. 2013; 110:E1685–94. [PubMed: 23589888]

23. Liebau S, Tischendorf M, Ansorge D, Linta L, Stockmann M, Weidgang C, et al. An inducible expression system of the calcium-activated potassium channel 4 to study the differential impact on embryonic stem cells. *Stem cells international*. 2011; 2011:456815. [PubMed: 21941566]
24. Lee YK, Ng KM, Lai WH, Chan YC, Lau YM, Lian Q, et al. Calcium homeostasis in human induced pluripotent stem cell-derived cardiomyocytes. *Stem Cell Rev*. 2011; 7:976–86. [PubMed: 21614516]
25. Zhang XH, Haviland S, Wei H, Saric T, Fatima A, Hescheler J, et al. Ca²⁺ signaling in human induced pluripotent stem cell-derived cardiomyocytes (iPS-CM) from normal and catecholaminergic polymorphic ventricular tachycardia (CPVT)-afflicted subjects. *Cell Calcium*. 2013; 54:57–70. [PubMed: 23684427]
26. Fatima A, Xu G, Shao K, Papadopoulos S, Lehmann M, Arnaiz-Cot JJ, et al. In vitro modeling of ryanodine receptor 2 dysfunction using human induced pluripotent stem cells. *Cell Physiol Biochem*. 2011; 28:579–92. [PubMed: 22178870]
27. Del Nido PJ, Glynn P, Buenaventura P, Salama G, Koretsky AP. Fluorescence measurement of calcium transients in perfused rabbit heart using rhod 2. *Am J Physiol*. 1998; 274:H728–41. [PubMed: 9486280]
28. Tallini YN, Ohkura M, Choi BR, Ji G, Imoto K, Doran R, et al. Imaging cellular signals in the heart in vivo: Cardiac expression of the high-signal Ca²⁺ indicator GCaMP2. *Proc Natl Acad Sci U S A*. 2006; 103:4753–8. [PubMed: 16537386]
29. Lin B, Kim J, Li Y, Pan H, Carvajal-Vergara X, Salama G, et al. High-purity enrichment of functional cardiovascular cells from human iPS cells. *Cardiovasc Res*. 2012; 95:327–35. [PubMed: 22673369]
30. Yang L, Soonpaa MH, Adler ED, Roepke TK, Kattman SJ, Kennedy M, et al. Human cardiovascular progenitor cells develop from a KDR⁺ embryonic-stem-cell-derived population. *Nature*. 2008; 453:524–8. [PubMed: 18432194]
31. Han L, Li Y, Tchao J, Kaplan AD, Lin B, Li Y, et al. Study familial hypertrophic cardiomyopathy using patient-specific induced pluripotent stem cells. *Cardiovasc Res*. 2014; 104:258–69. [PubMed: 25209314]
32. Choi BR, Salama G. Simultaneous maps of optical action potentials and calcium transients in guinea-pig hearts: mechanisms underlying concordant alternans. *J Physiol*. 2000; 529(Pt 1):171–88. [PubMed: 11080260]
33. Tallini YN, Brekke JF, Shui B, Doran R, Hwang SM, Nakai J, et al. Propagated endothelial Ca²⁺ waves and arteriolar dilation in vivo: measurements in Cx40BAC GCaMP2 transgenic mice. *Circ Res*. 2007; 101:1300–9. [PubMed: 17932328]
34. Salama G, Choi BR, Azour G, Lavasani M, Tumbev V, Salzberg BM, et al. Properties of new, long-wavelength, voltage-sensitive dyes in the heart. *J Membr Biol*. 2005; 208:125–40. [PubMed: 16645742]
35. Salama G, Hwang SM. Simultaneous optical mapping of intracellular free calcium and action potentials from Langendorff perfused hearts. *Curr Protoc Cytom*. 2009; Chapter 12(Unit 12):7.
36. Bett GC, Kaplan AD, Lis A, Cimato TR, Tzanakakis ES, Zhou Q, et al. Electronic “expression” of the inward rectifier in cardiocytes derived from human-induced pluripotent stem cells. *Heart Rhythm*. 2013; 10:1903–10. [PubMed: 24055949]
37. Kaplan AD, Lis A, Cimato TR, Tzanakakis ES, Zhou Q, Morales MJ, et al. Enhanced Differentiation of Stem Cell Derived Cardiac Myocytes by Electronic Expression of IK1 Reveals an Atrial-Specific Kv1.5-Like Current. *Biophysical journal*. 2014:631a. [PubMed: 24507603]
38. Ludwig A, Zong X, Stieber J, Hullin R, Hofmann F, Biel M. Two pacemaker channels from human heart with profoundly different activation kinetics. *Embo J*. 1999; 18:2323–9. [PubMed: 10228147]
39. Peters CJ, Chow SS, Angoli D, Nazzari H, Cayabyab FS, Morshedian A, et al. In situ co-distribution and functional interactions of SAP97 with sinoatrial isoforms of HCN channels. *J Mol Cell Cardiol*. 2009; 46:636–43. [PubMed: 19336273]
40. Difrancesco D, Noble D. The funny current has a major pacemaking role in the sinus node. *Heart Rhythm*. 2012; 9:299–301. [PubMed: 21925134]

41. DiFrancesco D, Ferroni A, Mazzanti M, Tromba C. Properties of the hyperpolarizing-activated current (I_f) in cells isolated from the rabbit sino-atrial node. *J Physiol*. 1986; 377:61–88. [PubMed: 2432247]
42. Frace AM, Maruoka F, Noma A. External K⁺ increases Na⁺ conductance of the hyperpolarization-activated current in rabbit cardiac pacemaker cells. *Pflugers Arch*. 1992; 421:97–9. [PubMed: 1326752]
43. Hoppe UC, Beuckelmann DJ. Characterization of the hyperpolarization-activated inward current in isolated human atrial myocytes. *Cardiovasc Res*. 1998; 38:788–801. [PubMed: 9747448]
44. O'Hara T, Rudy Y. Quantitative comparison of cardiac ventricular myocyte electrophysiology and response to drugs in human and nonhuman species. *Am J Physiol-Heart C*. 2012; 302:H1023–H30.
45. Lakatta EG, Maltsev VA, Vinogradova TM. A coupled SYSTEM of intracellular Ca²⁺ clocks and surface membrane voltage clocks controls the timekeeping mechanism of the heart's pacemaker. *Circ Res*. 2010; 106:659–73. [PubMed: 20203315]
46. Abramson JJ, Salama G. Sulfhydryl oxidation and Ca²⁺ release from sarcoplasmic reticulum. *Mol Cell Biochem*. 1988; 82:81–4. [PubMed: 3185520]
47. Zaidi NF, Lagenaur CF, Abramson JJ, Pessah I, Salama G. Reactive disulfides trigger Ca²⁺ release from sarcoplasmic reticulum via an oxidation reaction. *J Biol Chem*. 1989; 264:21725–36. [PubMed: 2532212]
48. Menshikova EV, Salama G. Cardiac ischemia oxidizes regulatory thiols on ryanodine receptors: captopril acts as a reducing agent to improve Ca²⁺ uptake by ischemic sarcoplasmic reticulum. *J Cardiovasc Pharmacol*. 2000; 36:656–68. [PubMed: 11065227]
49. Rottbauer W, Baker K, Wo ZG, Mohideen MA, Cantiello HF, Fishman MC. Growth and function of the embryonic heart depend upon the cardiac-specific L-type calcium channel alpha1 subunit. *Developmental cell*. 2001; 1:265–75. [PubMed: 11702785]
50. Nunes SS, Miklas JW, Liu J, Aschar-Sobbi R, Xiao Y, Zhang B, et al. Biowire: a platform for maturation of human pluripotent stem cell-derived cardiomyocytes. *Nature methods*. 2013; 10:781–7. [PubMed: 23793239]
51. Maltsev VA, Lakatta EG. The funny current in the context of the coupled-clock pacemaker cell system. *Heart Rhythm*. 2012; 9:302–7. [PubMed: 21925132]
52. Rosen MR, Nargeot J, Salama G. Point-counterpoint: The case for the funny current and the calcium clock. *Heart Rhythm*. 2011
53. Cerbai E, Sartiani L, DePaoli P, Pino R, Maccherini M, Bizzarri F, et al. The properties of the pacemaker current I_f in human ventricular myocytes are modulated by cardiac disease. *J Mol Cell Cardiol*. 2001; 33:441–8. [PubMed: 11181013]
54. Cerbai E, Mugelli A. I_f in non-pacemaker cells: role and pharmacological implications. *Pharmacol Res*. 2006; 53:416–23. [PubMed: 16713285]
55. Qu J, Altomare C, Bucchi A, DiFrancesco D, Robinson RB. Functional comparison of HCN isoforms expressed in ventricular and HEK 293 cells. *Pflugers Arch*. 2002; 444:597–601. [PubMed: 12194012]
56. Cerbai E, Pino R, Porciatti F, Sani G, Toscano M, Maccherini M, et al. Characterization of the hyperpolarization-activated current, I_f, in ventricular myocytes from human failing heart. *Circulation*. 1997; 95:568–71. [PubMed: 9024140]
57. Bucchi A, Baruscotti M, DiFrancesco D. Current-dependent block of rabbit sino-atrial node I_f channels by ivabradine. *J Gen Physiol*. 2002; 120:1–13. [PubMed: 12084770]
58. Loughrey CM, Otani N, Seidler T, Craig MA, Matsuda R, Kaneko N, et al. K201 modulates excitation-contraction coupling and spontaneous Ca²⁺ release in normal adult rabbit ventricular cardiomyocytes. *Cardiovasc Res*. 2007; 76:236–46. [PubMed: 17644079]
59. Takimoto E, Kass DA. Role of oxidative stress in cardiac hypertrophy and remodeling. *Hypertension*. 2007; 49:241–8. [PubMed: 17190878]
60. Kohler AC, Sag CM, Maier LS. Reactive oxygen species and excitation-contraction coupling in the context of cardiac pathology. *J Mol Cell Cardiol*. 2014; 73C:92–102. [PubMed: 24631768]
61. Ai X, Curran JW, Shannon TR, Bers DM, Pogwizd SM. Ca²⁺/calmodulin-dependent protein kinase modulates cardiac ryanodine receptor phosphorylation and sarcoplasmic reticulum Ca²⁺ leak in heart failure. *Circ Res*. 2005; 97:1314–22. [PubMed: 16269653]

Highlights

1. HiPS-CMs hold great promise for personalized medicine to treat cardiac diseases
2. The mechanisms underlying their automaticity remain unknown
3. Ventricular hiPS-CMs express HCN message but no significant funny current, I_f
4. Subcellular Ca^{2+} & V_m maps show that aberrant Ca^{2+} release precede depolarization
5. Stochastic subcellular Ca^{2+} waves control automaticity

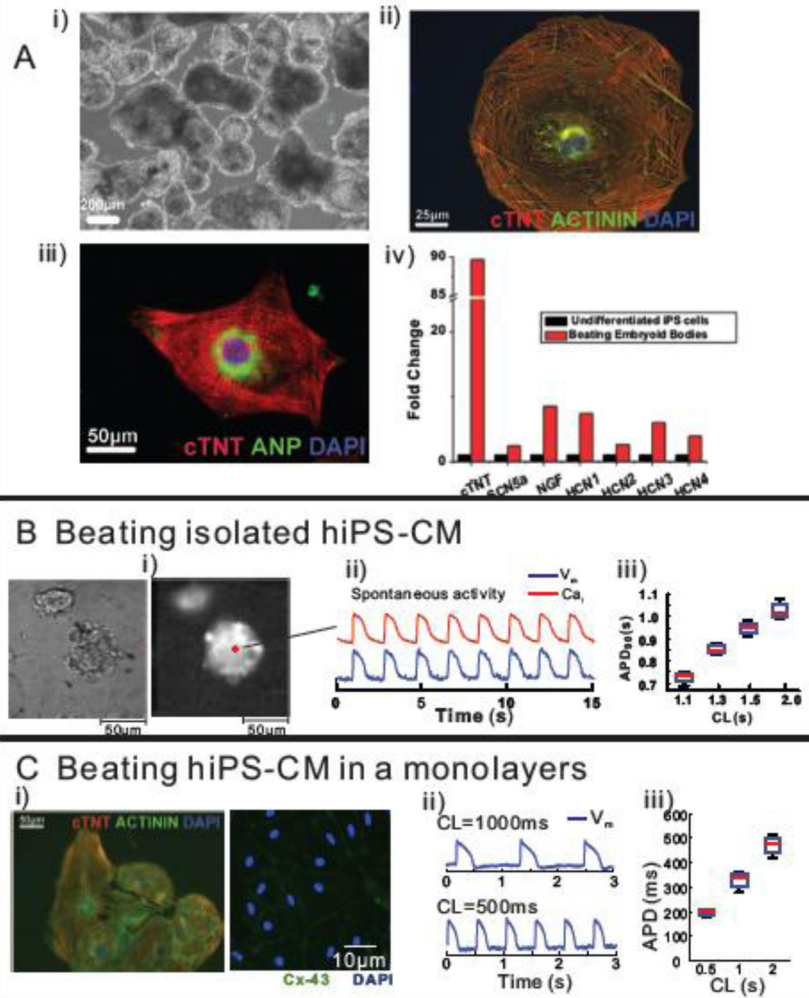


Figure 1. Characterization of iPS-derived cardiomyocytes

A: Immuno-staining of beating embryoid bodies of hiPS-CMs. i) a bright-field image, ii) immune-staining of CTNT (red), Actinin (green) and a nuclear stain, DAPI (blue), iii) immuno-staining of cardiac troponin T (CTNT, red), atrial natriuretic protein (ANP, green), a marker for late stage atrial or fetal CMs, and DAPI (blue) and iv) quantitative real time PCR using RNA isolated from undifferentiated hiPS cells and beating embryonic bodies of cardiac troponin T (cTNT), nerve growth factor (NGF) and the hyperpolarization activated cycling nucleotide gated channels (HCN 1 and 4) that underlie the pacemaker ‘funny’ current. Experiments were performed in triplicates.

B: Simultaneous measurement of intracellular Ca^{2+} (Ca_i) transients and V_m changes in embryoid bodies of hiPS-CMs. i) a bright-field (left) and a fluorescent image of PGH1 stained spontaneously beating embryoid bodies of hiPS-CMs, ii) simultaneous optical recording of Ca_i transients and membrane potential (V_m) changes at a marked pixel (pixel resolution= $1.5 \times 1.5 \mu\text{m}$), and iii) the relationship between action potential duration (APD) and cycle length (CL).

C: Immunolabeling and optical measurement of V_m changes in a spontaneously beating hiPS-CM monolayer. i) immunostaining of CTNT (red), actinin (green) and a nuclear stain,

DAPI (blue) (left) and connexins 43 (Cx-43, green) and a nuclear stain, DAPI (blue), ii) optical measurement of V_m changes, and iii) the relationship between APD and CL.

Author Manuscript

Author Manuscript

Author Manuscript

Author Manuscript

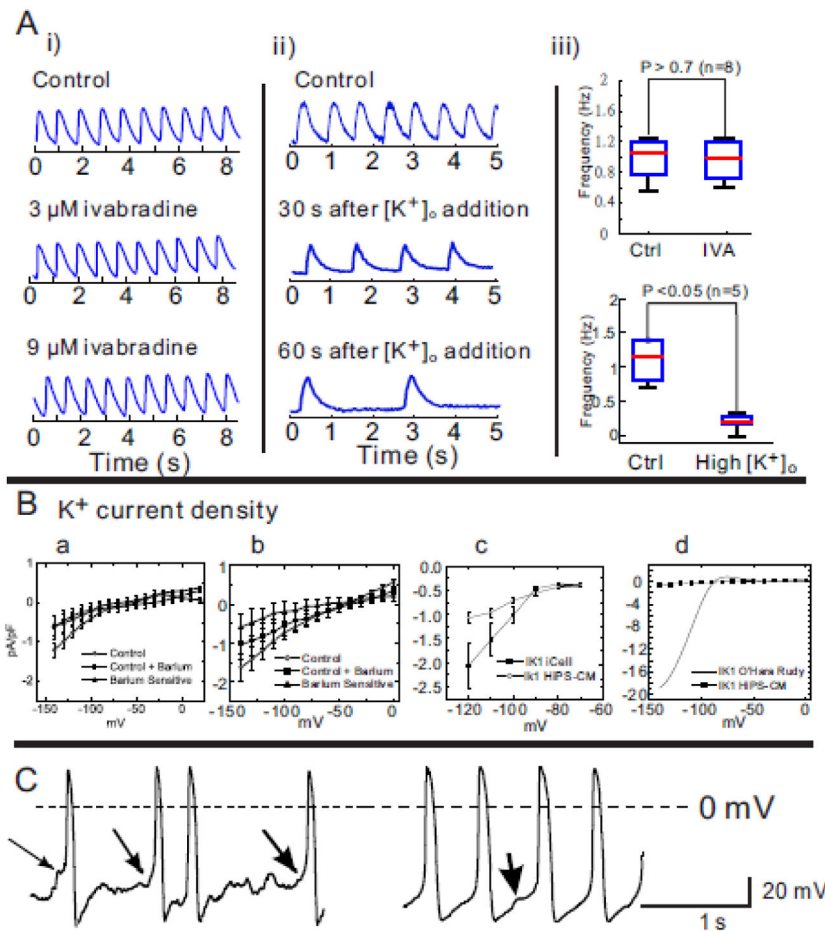


Figure 2. Pacemaker activity in dispersed hiPS-CMs

A: i) Ivabradine, an inhibitor of I_f , had no effect on spontaneous activity at concentrations of 3 and 9 μM even though the hiPS-CMs activity slowed down by increasing external $[\text{K}^+]_o$ from 4 to 8 mM. ii) An increase in extracellular K^+ from 4–8 mM decreased the rate of spontaneous activity in embryoid bodies ($n=5/5$). iii) Statistical comparison of spontaneous contraction in hiPS-CMs.

B: Early and late currents estimate a very small I_f and I_{K1} . Panel a: Current-to-voltage (I–V) plot of barium sensitive, insensitive and difference currents at the end of a 2000 ms pulse. Each data point represent the average of the current recorded in going from a holding potential of -40 mV to test potentials between -140 to 0 mV in steps of 10 mV. The cells were then treated with Ba^{2+} (1 mM) and the Ba^{2+} sensitive current was taken as the difference between the control and the Ba^{2+} treated current; $n=12$ hiPS-CMs (10 ventricular and 2 atrial). Panel b shows data from the same cells for peak inward current. Panel c: Current-to-voltage relationship of background currents surrounding EK for comparing relative magnitude of I_{K1} currents in iCell (Cellular Dynamics International) prepared hiPS-CMs versus scale preparation of hiPS-CMs in normal Tyrode's solution. Each data point represents the peak current recorded from -120 mV to -60 mV from a holding potential of -90 mV ($n=19$ and $n=10$ respectively). Panel d: Barium sensitive (early, from panel b, I_{K1}) currents in hiPS-CMs were compared to I_{K1} currents calculated for human ventricular

myocytes. The early barium sensitive current density per cell in panel B was plotted against the O'Hara Rudy model [44] for I_{K1} . Current density was normalized to cell capacitance and expressed in pA/pF.

C: Two examples of pacemaking activity in hiPS-CMs measured using whole cell recordings in the current-clamp mode. The first hiPS-CM (left) showed the typical "flat" period prior to initiation of an AP, with a preceding abrupt depolarization typical of a spontaneous Ca^{2+} -release event or a delayed afterdepolarization, DAD (arrows), the second (right) occurred less frequently and showed the appearance of pacemaker activity, even in such runs, spontaneous "DAD" behavior was noted (arrow). In this group, there were 11 ventricular, 4 atrial and 3 other cell type.

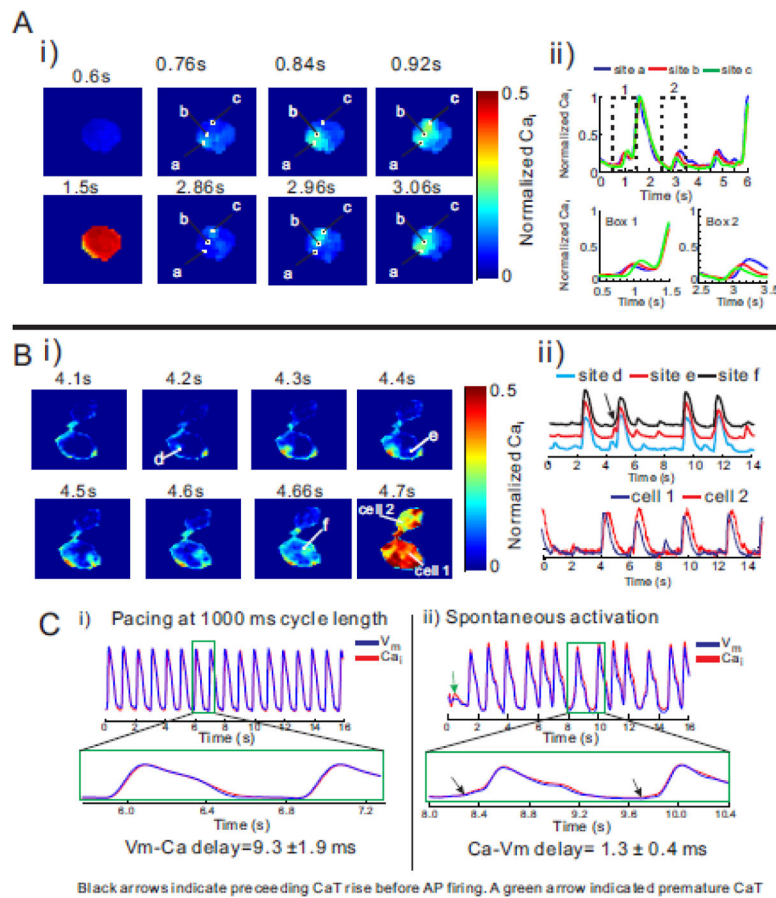


Figure 3. Subcellular Ca_i waves and spontaneous contractions in isolated hiPS-CMs

A: i) Maps of normalized Ca_i taken at different time-points reveal a sequence of subcellular Ca^{2+} release and local wave propagation occurring during diastole. The first subcellular Ca^{2+} release was initiated at site a (at 0.76s) and propagated to site b (0.84s) then c (0.92s) (see top panels) then a large synchronous SR Ca^{2+} release filled the cell at 1.5s. The next subcellular Ca_i elevation started near site c (2.86s), propagated c to b (2.96s) then to a (3.06s). Field of view was $50 \times 50 \mu m^2$. For GCaMP2 fluorescence, $\lambda_{excitation}$ was 480 ± 20 nm and $\lambda_{emission}$ was 510 ± 15 nm.

ii) Shows the time course of fluorescence traces of Ca_i recorded from sites a, b, and c at slow (top traces) and fast (bottom traces) sweep speeds. The superposition of Ca_i signals from sites a, b and c reveal the time-course and relative amplitude of subcellular waves. The small subthreshold local Ca_i elevations were typically 1/4 of the full amplitude of cellular CaTs. At fast sweep speed (Box 1), the subcellular Ca_i wave started at site 'a' and propagated to 'b' then 'c' before eliciting a CaT that produced a global Ca_i elevation throughout the cell (A, panel at 1500 ms). The next two sequences of subcellular Ca_i elevations started at site c (Box 2) and propagated to b then a; the sequence was repeated twice followed by a full size CaT.

B: i) Example of subcellular small amplitude Ca_i release that can dissipate and self-terminate or amplify to precede a global Ca_i release. A local Ca_i wave initiated at site 'e' propagated but self-terminated without producing a full size Ca_i transient. In contrast, a Ca_i

wave initiated at site 'f' propagated, was amplified and preceded a global Ca_i release. Field-of-view was $75 \times 75 \mu\text{m}^2$. ii) Optical traces of Ca_i recorded at site d, e, and f (top) and in two neighboring cells (bottom). Premature CaTs were unsynchronized but global CaTs were synchronized in these coupled cells with $\sim 100\text{ms}$ time delays.

C: Temporal delay between AP and Ca_i upstrokes. An ensemble of dispersed hiPS-CMs, optical APs and CaTs were simultaneously recorded. In (i), the cells were paced at 1 s cycle length resulting in the expected V_m to Ca_i coupling where V_m preceded Ca_i by 9.3 ± 1.9 ms. In contrast when the dispersed cells were not paced but exhibited spontaneous automaticity, Ca_i preceded V_m by 1 ± 0.4 ms, (n=5 preparations of dispersed cells).

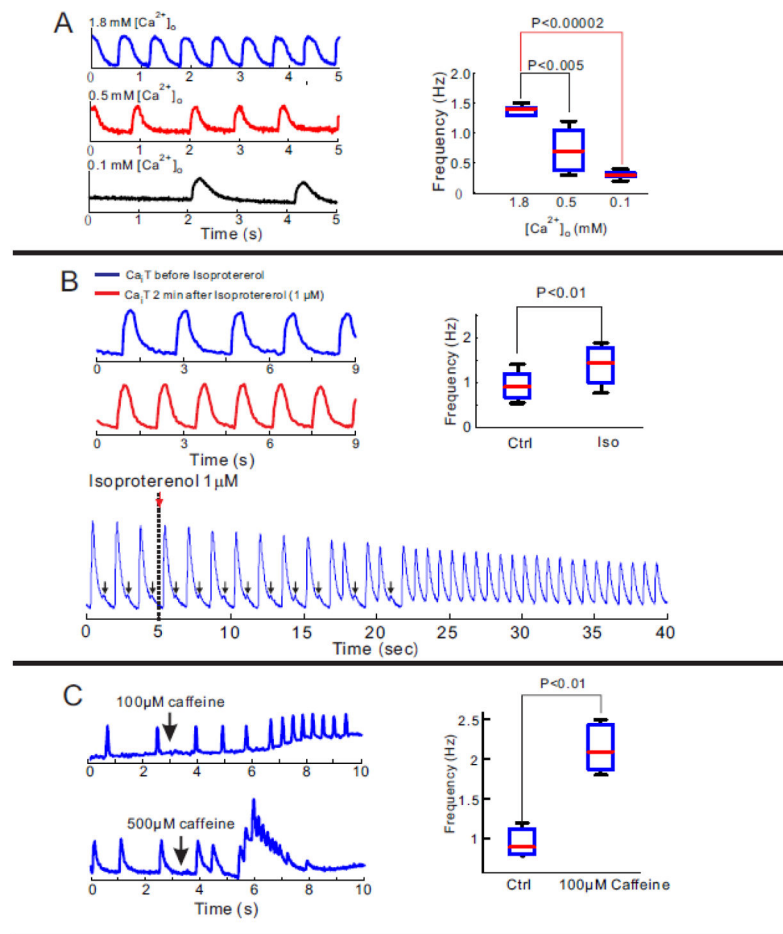


Figure 4. Modification of automaticity in hiPS-CMs by [Ca²⁺]_o titration and changes in RyR2 open probability

A: Frequency of intrinsic contractions is [Ca²⁺]_o dependent. The rate of spontaneous contractions in a cluster of hiPS-CMs is [Ca²⁺]_o dependent. Raising or lowering [Ca²⁺]_o from 0.5 mM, significantly increased or decreased the frequency of spontaneous contractions, respectively. Statistical analysis of the frequency of Ca_i transients demonstrated a tight correlation between frequency and [Ca²⁺]_o (right panel)

B: Chronotropic response of hiPS-CMs to β adrenergic stimulation. Infusion of 1 μM of isoproterenol significantly increases in frequency of spontaneous contraction in a cluster of hiPS-CMs (left traces). Statistical analysis of frequency of contractions for 5 preparations of iPS-CMs. Premature CaTs were gradually developed to full transients under 1 μM of isoproterenol administration.

C: Frequency of spontaneous contraction is caffeine sensitivity. After administration of 100 μM caffeine, spontaneous contraction of hiPS-CMs was gradually increased (left top panel). 500 μM of caffeine infusion emptied SR and stopped spontaneous contraction of hiPS-CMs (left bottom panel). Statistical comparison of frequency of spontaneous contraction before and after 100 μM caffeine infusion

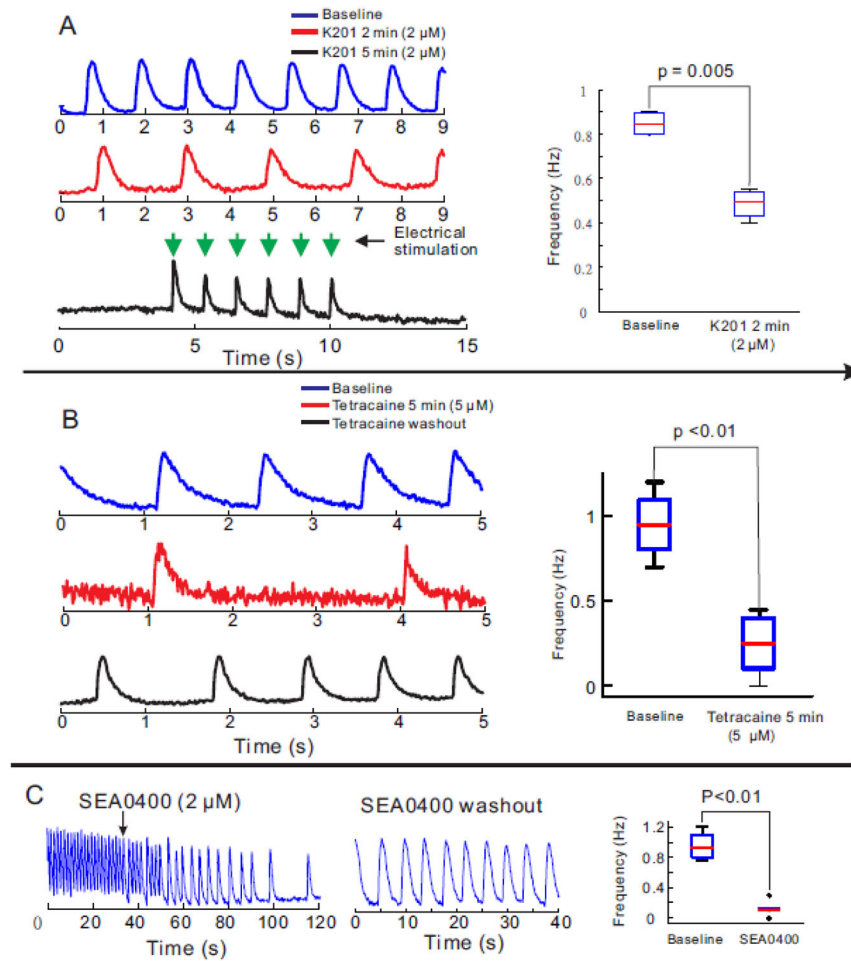


Figure 5. Manipulations of RyR2, and NCX and its efficacy on spontaneous contraction in hiPS-CMs

A: K201 (2 μ M), a selective RyR2 stabilizer gradually decreased the frequency of spontaneous contraction in a cluster of hiPS-CMs and eventually terminated spontaneous contraction (n=5/5). HiPS-CMs remained excitable by electrical stimulation. After 2 min of K201 exposure, a ~2-fold decrease in frequency of automaticity was statistically significant (right panel)

B: Similar effects of 5 μ M tetracaine infusion on spontaneous contraction in hiPS-CMs

C: SEA0400 (2 μ M), an inhibitor of the forward mode of NCX suppressed spontaneous contractions in a cluster of iPS-CMs; an effect that was reversible by washing out SEA0400 (right trace) (n=4/4).

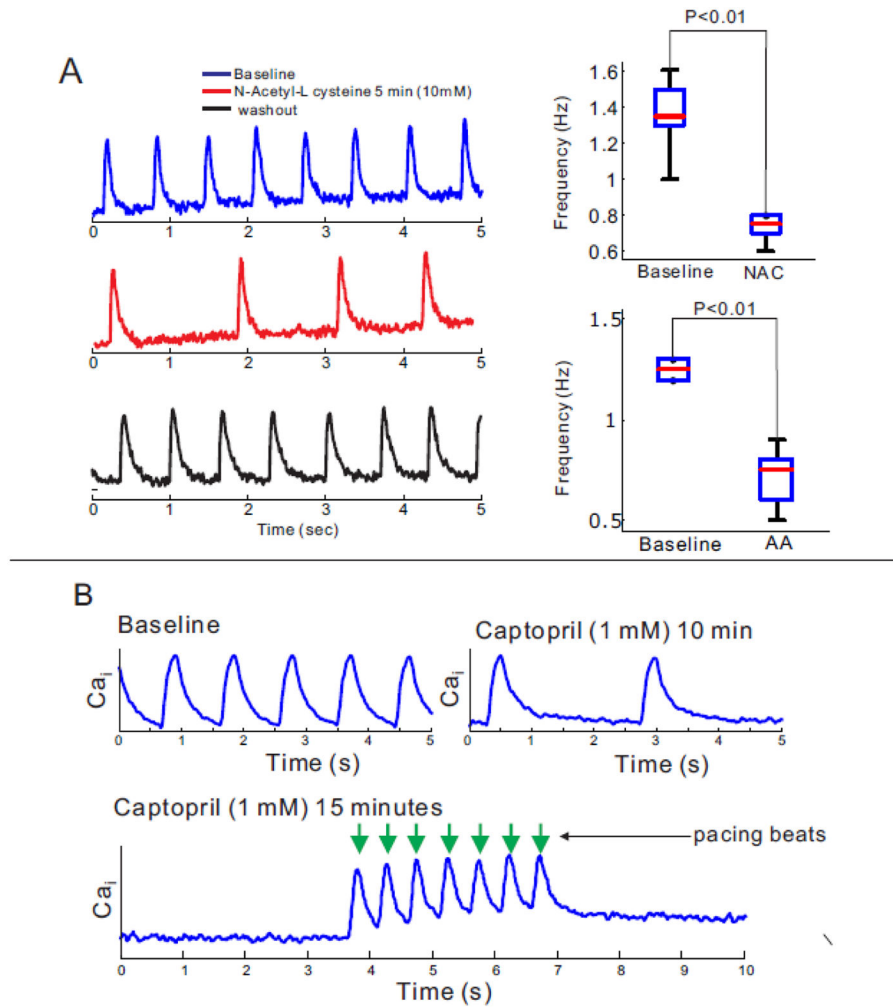


Figure 6. Modification of automaticity in hiPS-CMs by RyR2 redox state

A: Anti-oxidant agents, N-Acetyl-L-Cysteine (NALC) and ascorbic acid (AA) significantly reduced automaticity of hiPS-CMs (n=10).

B: The membrane permeable thiol reducing agent, captopril (1 mM) slowed-down the rate of spontaneous contractions in 10 min (top trace) and stopped automaticity within 15 min (n=3/6). Contractions of iPS-CMs rendered quiescent by captopril were triggered by electrical stimuli (arrows).

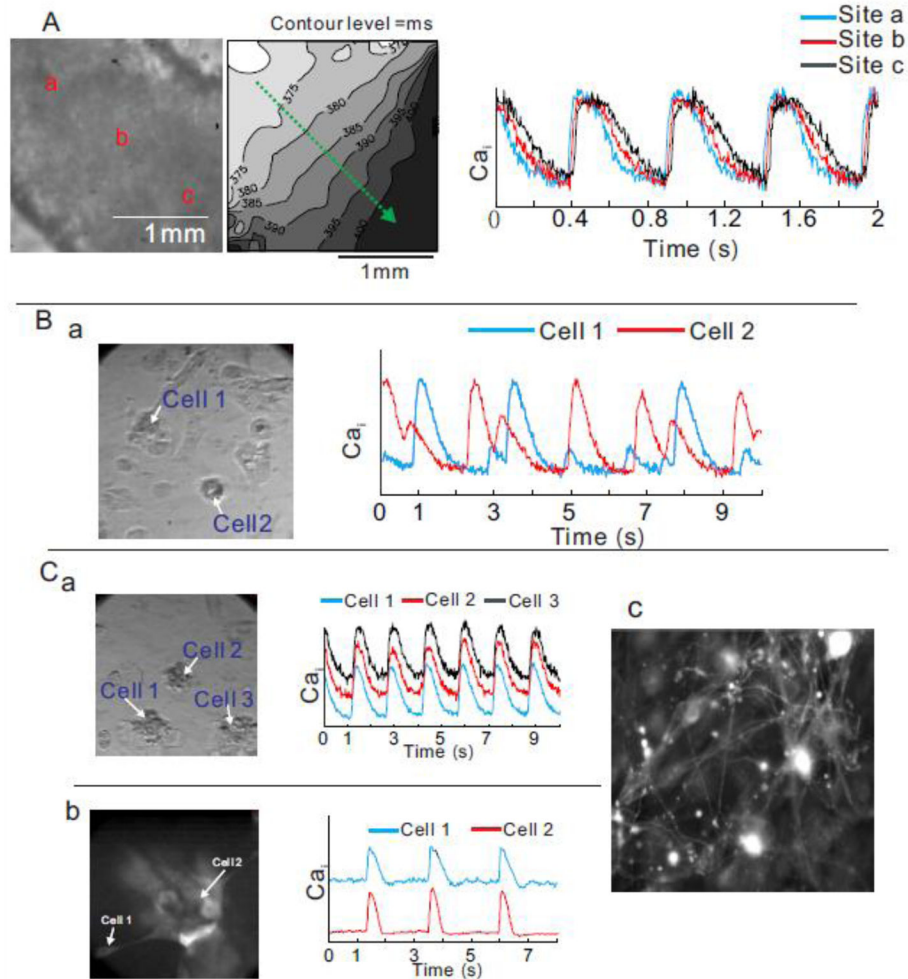


Figure 7. Intercellular communication

A: Propagation of spontaneous contraction in a dense cluster of hiPS-CMs. A left panel is a picture of a cluster. A middle panel is an activation map. A green arrow indicates the direction of propagation. A right panel shows superimposed calcium traces at site a, b, and c.

B: Unsynchronized and irregular contraction in remote hiPS-CMs. A picture of sparsely distributed hiPS-CMs (left panel). Superimposed calcium traces from cells 1 and 2 (right panel).

C: Intercellular synchronization of contraction between a cluster and satellite hiPS-CMs connected to each other via microfiber. Panel a) shows a picture of remote hiPS-CMs (left panel) and superimposed Ca_i traces of cells 1, 2 and 3 (right traces). Another example of synchronization is shown through a fluorescence image of membrane-bound voltage-sensitive dye (PGH1) (panel b) and Ca_i traces of a cluster and a satellite hiPS-CMs. A high-resolution fluorescence image of a cluster of hiPS-CMs using a membrane-bound dye reveals a complex network of microfibers that underlie intercellular coupling among CMs that are far apart (30–50 μm) (panel c). All panels have dimensions of 150 $\mu\text{m} \times 150 \mu\text{m}$.

Table 1

List of primers used for RT-PCR

	Forward	Reverse
Cyclophilin	CATCTGCACTGCCAAGACTGA	TTCATGCCTTCTTCACTTTGC
cTNNT2	AGCCCAGGTCGTTTCATGCC	GCCTCGATCAGCGCCTGCAA
SCN5A	TCACTCGTCTTCAACATGC	AGGTGTAATGGCGGTGAAG
NGF	GAGCGCAGCGAGTTTTGGCC	ATGCACCTCAGTGTGGCCAG
HCN4	CGCATTGGCAAGAAGAACTCCA	AGTGGGCCATCTCCCGGTCAT
HCN1	GCCATGCTGAGCAAGTTGAG	TCAGCAGGCAAATCTCTCCA
HCN2	AGCGACTTCAGGTTCTACTGG	ACCACGTGCGCAGATACTTC
HCN3	CAAATCTGGGCCTGAGCCTA	CAGGTCCCAGTAAAACCGGA

Author Manuscript

Author Manuscript

Author Manuscript

Author Manuscript